

Bayesian biclustering for microbial metagenomic sequencing data via multinomial matrix factorization

FANGTING ZHOU ^{1,2}, KEJUN HE ^{2,*}, QIWEI LI ³, ROBERT S. CHAPKIN ⁴, YANG NI ^{1,*}

¹ Department of Statistics, Texas A&M University, College Station, Texas, U.S.A.

² Institute of Statistics and Big Data, Renmin University of China, Beijing, China

³ Department of Mathematical Sciences, The University of Texas at Dallas, Dallas, Texas, U.S.A

⁴ Department of Nutrition and Food Science, Texas A&M University, College Station, Texas,

U.S.A

kejunhe@ruc.edu.cn, yni@stat.tamu.edu

SUMMARY

High-throughput sequencing technology provides unprecedented opportunities to quantitatively explore human gut microbiome and its relation to diseases. Microbiome data are compositional, sparse, noisy, and heterogeneous, which pose serious challenges for statistical modeling. We propose an identifiable Bayesian multinomial matrix factorization model to infer overlapping clusters on both microbes and hosts. The proposed method represents the observed over-dispersed zero-inflated count matrix as Dirichlet-multinomial mixtures on which latent cluster structures are built hierarchically. Under the Bayesian framework, the number of clusters is automatically determined and available information from a taxonomic rank tree of microbes is naturally incorporated, which greatly improves the interpretability of our findings. We demonstrate the utility

*To whom correspondence should be addressed.

of the proposed approach by comparing to four alternative methods in simulations. An application to a human gut microbiome dataset involving patients with inflammatory bowel disease reveals interesting clusters, which contain bacteria families *Bacteroidaceae*, *Bifidobacteriaceae*, *Enterobacteriaceae*, *Fusobacteriaceae*, *Lachnospiraceae*, *Ruminococcaceae*, *Pasteurellaceae*, and *Porphyromonadaceae* that are known to be related to the inflammatory bowel disease and its subtypes according to biological literature. These bacteria families can become potential targets for microbiome-based treatment of the inflammatory bowel disease.

Key words: Bayesian nonparametric prior; Compositional data analysis; Mixture model; Phylogenetic Indian buffet process.

1. INTRODUCTION

Microbes parasitic on various parts of the human body are inseparable from the well-being of their host. Recent studies have shown that microbiota have profound effects on the formation, development, and progression of numerous pathologies like psoriasis (Benhadou *and others*, 2018), obesity (Castaner *and others*, 2018), inflammatory bowel disease (IBD, Franzosa *and others*, 2019), preterm birth (Fettweis *and others*, 2019), and diabetes (Tilg and Moschen, 2014). In this article, we focus on IBD, a chronic and complex disease that features heterogeneity at the microbiome level. As Lloyd-Price *and others* (2019) pointed out, the disease activity is accompanied by molecular disruptions in microbial transcription, variations with taxonomic shifts, and other genomic activities. The seemingly strong association between gut microbes and IBD urges scientists to investigate microbial composition profiles in patients, which can improve our understanding of disease causes and potentially lead to precise treatments.

The emergence of high-throughput sequencing technology such as deep metagenomic sequencing has generated a plethora of data that have enabled researchers to quantitatively study both

taxonomic and functional effect of microbiota on hosts (Turnbaugh *and others*, 2007). However, due to the compositional, sparse, heterogeneous, and noisy nature of the microbiome abundance data, they pose serious challenges in statistical modeling.

Composition. Microbiome abundance data are inherently compositional (Gloor *and others*, 2017), in the sense that individual counts are restricted by the extracted sample and assay technique. The abundance of each microbial component is only coherently interpretable relative to others within that sample. As a consequence, models that treat microbial taxa as independent variables may lead to substantial biases (Buccianti, 2013).

Sparsity. Microbial counts are sparse. Taking our IBD data as an example, more than 45% of the observations are exact zeros, which greatly complicates the sampling distribution. Excessive zeros occur mainly for two reasons: (i) bacteria are not present in tested hosts and hence the zeros are true biological zeros, and (ii) the sequencing depth is not enough to capture rare bacteria which is referred to as technical zeros. Often, approaches need to explicitly differentiate between these two types of zeros to reduce estimation biases, which are addressed by the two-part model, the tobit model, and their combination (Liu *and others*, 2019).

Heterogeneity. The composition of microbiota is heterogeneous and drastically different across hosts. Methods based on iid sampling are deemed unsuitable for microbiome data analysis. Individualized characterization is necessary to unravel genuine information and avoid spurious conclusions derived from a homogeneous modeling assumption.

Noisiness. Measurements from sequencing platforms contain high levels of noises due to the technical instability, which inevitably confounds with the biological variation that researchers strive to investigate. Methods that ignore the experimental noises are susceptible to false discoveries which will be propagated to downstream analysis and hinder scientific advancement.

Current statistical methodologies in the analysis of microbiome data are largely based on the regression framework. For example, in regression analysis where covariates are compositional, the

linear log-contrast model with ℓ_1 regularization was adopted in Lin *and others* (2014) and Shi *and others* (2016) to select relevant covariates in the analysis of metagenomic data. However, they do not explicitly take into account the excessive zeros but replace them with arbitrary small numbers. When treating compositional data as response, a sparse Dirichlet-multinomial regression model was employed in Chen and Li (2013) to associate microbiome composition with environmental covariates. The method is able to account for over-dispersion of observed counts and select important variables. Chen and Li (2016) proposed a zero-inflated Beta regression model. The model includes a logistic regression component to model presence or absence of microbes in samples and a Beta regression component to model non-zero microbiome abundance.

There are also a rising number of models focusing on revealing microbiome interactions. For example, Friedman and Alm (2012) proposed to estimate the Pearson correlations between log-transformed components of compositional data under the assumption of sparsity, which is later implemented more efficiently with parallel computing by Watts *and others* (2018). A composition-adjusted thresholding was proposed by Cao *and others* (2019a) to obtain a sparse correlation estimate. More recently, Cai *and others* (2019) developed a Markov random field model to detect differential microbial networks. A key step in their approach is to dichotomize microbial compositions into a binary matrix. However, the dichotomization in their approach is based on a fixed quantile, the choice of which is somewhat arbitrary and sensitive.

While the majority of microbiome data analyses are performed in a supervised manner, in this paper we focus on an unsupervised learning task, namely, the probabilistic matrix factorization of microbiome data which can also be interpreted as overlapping biclustering. Many matrix factorization techniques have been proposed to handle continuous matrices (Bhattacharya and Dunson, 2011; Ročková and George, 2016), non-negative matrices (Lee and Seung, 2000; Hoyer, 2004), count matrices (Zhou *and others*, 2012; Gopalan *and others*, 2014), and binary matrices (Meeds *and others*, 2007; Ni *and others*, 2019b; Wu *and others*, 2019). However, none of these

methods is directly applicable to compositional microbiome data. Recently, a low rank approximation method was proposed by Cao *and others* (2019b) which is directly applicable to microbiome composition. Their method is an optimization approach that minimizes the multinomial likelihood-based loss function combined with a nuclear norm regularization on the composition matrix. They focused on recovering the composition and matrix factorization rather than inferring latent clustering structure which is the main objective of this paper. Xu *and others* (2020) developed a zero-inflated Poisson factor model with Poisson rates negatively related to inflated zero occurrences. Again, their main focus was on reducing the dimensionality of the microbiome data and a separate clustering algorithm is required to identify the clusters.

In this paper, we propose a Bayesian multinomial matrix factorization (MMF) model that infers the latent clustering structure from compositional, sparse, heterogeneous, and noisy microbiome data. The proposed MMF introduces a mixture model representation of observations through a set of latent variables to indicate the relative abundance of taxa. In essence, this simple formulation of the sampling model *adaptively* dichotomizes the multinomial observations into a binary matrix, which is more robust to noise and does not require a separate treatment of excessive zeros. Given the binary indicator matrix, priors are imposed hierarchically to characterize the heterogeneity via latent features. Specifically, we construct the hierarchical model with a combination of latent logit model, phylogenetic Indian buffet process prior (pIBP, Miller *and others*, 2008; Chen *and others*, 2016), and beta-Bernoulli prior. Using pIBP, we are able to infer an unknown number of overlapping clusters/communities of the taxa. pIBP also takes into account the taxonomic relationships among the taxa, which gives rise to more interpretable and reliable results. Conditional on the clusters of taxa, the beta-Bernoulli prior are assigned to cluster hosts, again allowing overlaps. Moreover, the sparse nature of the pIBP and beta-Bernoulli priors leads to an identifiable matrix factorization. Using simulations, we demonstrate that the proposed MMF has favorable performance compared to competing methods and is relatively ro-

bust to the choice of hyperparameters and misspecified tree information. We then apply MMF to an IBD microbiome dataset (Qin *and others*, 2010), which reveals interesting clusters containing bacteria families *Bacteroidaceae*, *Bifidobacteriaceae*, *Enterobacteriaceae*, *Fusobacteriaceae*, *Lachnospiraceae*, *Ruminococcaceae*, *Pasteurellaceae*, and *Porphyromonadaceae* that are known to be related to the IBD and its subtypes according to biological literature. These bacteria families can become potential targets for microbiome-based treatment of the IBD.

The rest of this paper is organized as follows. We introduce the proposed MMF model in Section 2. Posterior inference based on Markov chain Monte Carlo (MCMC) sampling is described in Section 3. In Sections 4 and 5, we respectively illustrate our approach with simulation studies and the analysis of an IBD dataset. This paper is concluded with a brief discussion in Section 6.

2. MODEL

2.1 *Classifying Taxon Abundance via Adaptive Dichotomization*

Let x_{ij} denote the observed count of taxon j in host i , $j = 1, \dots, p$ and $i = 1, \dots, n$. Let $\mathbf{x}_i = (x_{i1}, \dots, x_{ip})^\top$ and $N_i = \sum_{j=1}^p x_{ij}$. We assume \mathbf{x}_i follows a Dirichlet-multinomial distribution,

$$\mathbf{x}_i \sim \text{Multinomial}(N_i, \boldsymbol{\pi}_i)$$

with host-specific relative abundances,

$$\boldsymbol{\pi}_i = (\pi_{i1}, \dots, \pi_{ip})^\top \sim \text{Dirichlet}(\boldsymbol{\eta}_i),$$

where $\boldsymbol{\eta}_i = (\eta_{i1}, \dots, \eta_{ip})^\top$. Note that the Dirichlet-distributed relative abundances $\boldsymbol{\pi}_i$ can be equivalently represented as normalized gamma random variables $\boldsymbol{\pi}_i = \boldsymbol{\gamma}_i / \sum_{j=1}^p \gamma_{ij}$ with unnormalized relative abundances $\boldsymbol{\gamma}_i = (\gamma_{i1}, \dots, \gamma_{ip})^\top$ and $\gamma_{ij} \stackrel{\text{ind}}{\sim} \text{Gamma}(\eta_{ij}, 1)$.

We introduce a latent indicator variable z_{ij} to classify whether a taxon j is significantly *present* or *absent* in host i . There is no consensus on the classification of taxa based on absolute or relative abundances. In supervised tasks, the classification rule may be chosen to minimize

certain objective functions. For example, when the goal is to predict a response variable with microbiome covariates, one can potentially find an optimal dichotomization that minimizes the prediction error. Lack of such golden standard in matrix factorization, we propose a mixture model to probabilistically classify raw taxa counts into states of high presence or absence,

$$\gamma_{ij} \sim z_{ij}\text{Gamma}(s_j, 1) + (1 - z_{ij})\text{Gamma}(t_j, 1) \quad \text{with } s_j > t_j. \quad (2.1)$$

In words, due to the constraint $s_j > t_j$, $z_{ij} = 1$ indicates high relative abundance and $z_{ij} = 0$ indicates low relative abundance. The zero counts would naturally fall into the latter category with high probability. The induced distribution of \mathbf{x}_i is a discrete mixture of Dirichlet-multinomial distributions with 2^p components, with each component corresponding to one configuration of $(z_{i1}, \dots, z_{ip})^\top$. The latent variable z_{ij} can be viewed as a denoised version of the raw observations x_{ij} . A similar idea was recently used by Cai *and others* (2019) where they adopted a fixed 0.25 quantile as a hard cutoff to dichotomize microbiome data. Our approach differs from theirs in that we do not need to fix a cutoff and the proposed method adaptively dichotomizes the data. We assign hyperpriors on the unknown parameters (s_j, t_j) ,

$$p(s_j, t_j) = \text{Gamma}(s_j | \alpha_s, \beta_s) \times \text{Gamma}(t_j | \alpha_t, \beta_t) \times \mathbf{I}(s_j > t_j), \quad (2.2)$$

with $\alpha_s = \alpha_t = \alpha = 1$ and $\beta_s = \beta_t = \beta = 0.1$. Sensitivity analyses will be performed on the choice of these hyperparameters in Section 4 and Supplementary Material (Section B).

The mixture model in (2.1) can reliably classify taxa with well separated relative abundances into two states. However, the classification can have greater uncertainties for taxa with less variable relative abundances across observations. In Section 2.2, we will introduce latent structures on $\mathbf{Z} = (z_{ij})$ that stabilize uncertain classifications, reduce the dimensionality, and induce overlapping cluster structure for both hosts and microbial taxa.

2.2 Biclustering Taxa and Hosts via Binary Matrix Factorization

We introduce lower-dimensional matrices to characterize the heterogeneity of both rows and columns of \mathbf{Z} . In particular, we let $\mathbf{A} = (a_{ik}) \in \{0, 1\}^{n \times K}$ and $\mathbf{B} = (b_{jk}) \in \{0, 1\}^{p \times K}$ denote the host-cluster and taxon-cluster matrices with K clusters. The clustering interpretations of \mathbf{A} and \mathbf{B} will be elaborated in Section 2.3. The number K of columns of \mathbf{A} and \mathbf{B} is usually much smaller than the dimensions of the original data (n and p). We link \mathbf{A} and \mathbf{B} to z_{ij} by a latent logit model

$$\text{logit}\{\Pr(z_{ij} = 1)\} = c_j + \sum_{k=1}^K a_{ik} w_{jk} b_{jk}, \quad (2.3)$$

where $\text{logit}(p) = \log\{p/(1-p)\}$. If a group of hosts have a common activated biological pathway (related to normal body functions or diseases) that involves a common set of taxa, then these taxa are likely to have significant presence in those host samples. Therefore, we choose to constrain w_{jk} to be positive, although in principle they can take any values; similar considerations in a different context were made in Wood *and others* (2006). Parameter c_j represents the baseline probability of the presence of taxon j . We assume weakly informative priors on w_{jk} and c_j , $w_{jk} \sim \text{Gamma}(\alpha_w, \beta_w)$, $c_j \sim \text{N}(\mu_c, \sigma_c)$, with $\mu_c = 0$, $\sigma_c = 100$, $\alpha_w = 1$, and $\beta_w = 0.1$.

2.3 Indian Buffet Process and Taxonomic Rank Tree

The host-cluster matrix \mathbf{A} and taxon-cluster matrix \mathbf{B} can be interpreted as clustering of rows and columns of \mathbf{Z} , respectively. Host i (taxon j) belongs to cluster k if the corresponding $a_{ik} = 1$ ($b_{jk} = 1$). Since we do not constrain \mathbf{A} and \mathbf{B} to having unit row sums, clusters can have overlaps. This is useful in microbiome applications because a taxon can be active in multiple communities and likewise a host can also belong to more than one group. To make inference on these two matrices, we will impose a Bayesian nonparametric prior on \mathbf{B} that can automatically determine the number K of clusters.

The Indian buffet process (IBP, Griffiths and Ghahramani, 2005) has been widely used as a

Bayesian nonparametric prior on binary matrices with potentially unbounded number of columns. IBP assumes the rows of the binary matrix are exchangeable. This assumption becomes a limitation when the rows (taxa) are seemingly dependent as in our case. For instance, the relationships between taxa are commonly organized as a taxonomic rank tree. Taxa with smaller distances on the tree tend to have similar biological functions and therefore are expected to have higher probability of being in the same cluster. To incorporate this prior knowledge, we adopt the phylogenetic IBP (pIBP, Miller *and others*, 2008) to encourage taxonomically similar taxa to form clusters.

To describe the generating process of pIBP, we first assume a fixed and finite number \tilde{K} of clusters and will later relax it. Conditional on \tilde{K} , we associate a parameter p_k to each column of \mathbf{B} , which is assigned a Beta($\alpha/\tilde{K}, 1$) prior. We put a Gamma(1, 1) prior on α to infer its value from data. While the columns of \mathbf{B} are still independent as in IBP, entries within each column are generated jointly, with the pattern of dependence characterized by a stochastic process on a taxonomic rank tree. The tree has p taxa of interest as leaves and higher taxonomic ranks as internal/root nodes. Assume the path from every leaf up to the root contains $(L - 1)$ internal nodes, and each edge has length $l = 1/L$ so that the total length of the path from every leaf to the root is 1. This implies that the marginal prior probability of $b_{jk} = 1$ is the same across taxa $j = 1, \dots, p$.

To generate the entries of the k th column, we proceed as follows: i) assign value zero to the root node of the tree; ii) along any path from the root to a leaf, let the value change to one with an exponential rate $r_k l$ where $r_k = -\log(1 - p_k)$; iii) once the value has changed to one along a path from the root, all leaves below that change point are assigned value one; and iv) set the entries in the k th column of \mathbf{B} to the values of the corresponding leaves. By construction, leaves that are closer on the tree tend to receive identical values (of zeros or ones) in each column and therefore the corresponding taxa are more likely to fall in the same cluster. Note that the marginal prior

probability of $b_{jk} = 1$ is p_k , as given in the original paper of Miller *and others* (2008). To remove the dependency of the generating process from a fixed \tilde{K} , we let \tilde{K} go to infinity and obtain the pIBP. Hereafter we omit empty columns and denote the number of non-empty columns by K .

Conditional on taxon-cluster matrix \mathbf{B} (only via K), each element a_{ik} in \mathbf{A} follows an independent beta-Bernoulli distribution $a_{ik} \stackrel{\text{iid}}{\sim} \text{Bernoulli}(\rho)$, and $\rho \sim \text{Beta}(\alpha_\rho, \beta_\rho)$ with $\alpha_\rho = \beta_\rho = 1$. The complete model is summarized in Table 1.

2.4 Identifiability of the Proposed Model

Matrix factorization is often non-identifiable without additional assumptions. For example, model (2.3) can be written in a matrix form,

$$\mathbf{Q} = \mathbf{C} + \mathbf{A}\mathbf{B}^\top,$$

where $\mathbf{Q} = [q_{ij}]_{ij}$ with $q_{ij} = \text{logit}\{\text{Pr}(z_{ij} = 1)\}$, $\mathbf{C} = \mathbf{1}_p \mathbf{c}^\top$ with $\mathbf{1}_p = (1, \dots, 1)^\top$ and $\mathbf{c} = (c_1, \dots, c_p)^\top$, and, slightly abusing the notation, $\mathbf{B} = [w_{jk} b_{jk}]_{jk}$ absorbs the weights w_{jk} . Let $\tilde{\mathbf{A}} = \mathbf{A}\mathbf{P}$ and $\tilde{\mathbf{B}} = \mathbf{B}\mathbf{P}$ for any $K \times K$ orthogonal matrix \mathbf{P} . It is obvious that $\tilde{\mathbf{A}}\tilde{\mathbf{B}}^\top = \mathbf{A}\mathbf{P}\mathbf{P}^\top\mathbf{B}^\top = \mathbf{A}\mathbf{B}^\top$. Consequently, (\mathbf{A}, \mathbf{B}) and $(\tilde{\mathbf{A}}, \tilde{\mathbf{B}})$ would lead to the same \mathbf{Q} and the same sampling distribution, and are therefore non-identifiable in general. However, the fact that \mathbf{A} is binary makes the proposed matrix factorization identifiable up to column permutations.

Since the orthogonal matrix preserves lengths and angles of vectors, and \mathbf{A} and $\tilde{\mathbf{A}}$ are binary matrices, it holds that \mathbf{A} and $\tilde{\mathbf{A}}$ have the same number of ones in each row and have the same co-occurrence of ones for any pair of rows,

$$\begin{aligned} \#\{k : \tilde{a}_{ik} = 1\} &= \sum_{k=1}^K \tilde{a}_{ik}^2 = \sum_{k=1}^K a_{ik}^2 = \#\{k : a_{ik} = 1\}, \quad i = 1, \dots, n, \\ \#\{k : \tilde{a}_{ik} = \tilde{a}_{sk} = 1\} &= \sum_{k=1}^K \tilde{a}_{ik} \tilde{a}_{sk} = \sum_{k=1}^K a_{ik} a_{sk} = \#\{k : a_{ik} = a_{sk} = 1\}, \quad i \neq s. \end{aligned}$$

These two equalities imply that \mathbf{A} and $\tilde{\mathbf{A}}$ are column permutations to each other.

3. POSTERIOR INFERENCE

The proposed MMF is parameterized by $\{\mathbf{A}, \mathbf{B}, \mathbf{Z}, \{\gamma_i\}_{i=1}^n, \{\mathbf{w}_j, c_j, s_j, t_j\}_{j=1}^p, \{p_k\}_{k=1}^K, \alpha, \rho\}$. We carry out the posterior inference by MCMC simulation. To improve mixing, we marginalize out unnormalized relative abundance parameters γ_i 's. While other parameters are trivial to update with Gibbs or Metropolis-Hasting (M-H), care must be taken in updating \mathbf{B} and $\{p_k\}_{k=1}^K$, details of which are provided below. The updating procedures of other parameters are presented in the Supplementary Material (Section A). We let \mathbf{b}_k and \mathbf{b}_k^{-j} respectively denote the k th column of \mathbf{B} and the k th column of \mathbf{B} without the j th entry. Sequentially for $j = 1, \dots, p$, we cycle through the following three steps.

Step i. Update existing (non-empty) columns $k = 1, \dots, K$ of \mathbf{B} . For $j = 1, \dots, p$, we sample the binary b_{jk} from the full conditional distribution,

$$p(b_{jk}|\cdot) \propto p(b_{jk}|\mathbf{b}_k^{-j}, p_k) \prod_{i=1}^n p(z_{ij}|\{a_{ik}, b_{jk}, w_{jk}\}_{k=1}^K, c_j).$$

While an analytic form of $p(b_{jk}|\mathbf{b}_k^{-j}, p_k)$ is hard to obtain, it can be computed by the sum-product algorithm exactly and efficiently. Details of the sum-product algorithm can be found in Bishop (2006). Importantly, if a column becomes all zeros after update, we delete that column and reduce K by 1.

Step ii. Update p_k for existing columns of \mathbf{B} . Suppose b_{jk} is any non-zero entry in the k th column. The full conditional of p_k is given by

$$p(p_k|\mathbf{b}_k, \alpha) \propto p(p_k|b_{jk}, \alpha) p(\mathbf{b}_k^{-j}|p_k, b_{jk}),$$

where the first factor is a standard uniform distribution (Miller *and others*, 2008) and the second factor can be efficiently computed by decomposing it into a series of univariate conditional distributions using chain rule. For example, without loss of generality,

assuming $j = 1$, then

$$p(\mathbf{b}_k^{-1}|p_k, b_{1k}) = p(b_{2k}|p_k, b_{1k}) p(b_{3k}|p_k, b_{1k}, b_{2k}) \cdots p(b_{pk}|p_k, b_{1k}, \dots, b_{p-1,k}),$$

where each factor can be computed again using the sum-product algorithm. Since we only know the full conditional up to a normalization constant, we draw p_k by a M-H step, where a new value is proposed from $p_k^* \sim q(p_k^*|p_k) = N(p_k, \sigma_k^2)$ and is accepted with probability

$$\min \left\{ 1, \frac{q(p_k|p_k^*) p(\mathbf{b}_k^{-j}|p_k^*, b_{jk})}{q(p_k^*|p_k) p(\mathbf{b}_k^{-j}|p_k, b_{jk})} \mathbf{I}(p_k^* \in [0, 1]) \right\}.$$

Following the default choice in Miller *and others* (2008), we choose $\sigma_k = cp_k(1-p_k) + \delta$, with $c = 0.06$ and $\delta = 0.08$.

Step iii. Propose new columns. After all the existing columns are updated, we propose to add new columns. We first draw

$$K^* \sim \text{Poisson}(\alpha \{\psi(l^* + l + 1) - \psi(l^* + 1)\}),$$

where $\psi(\cdot)$ is the digamma function, $l^* = (P - 2)l$, and P is the total number of nodes in the tree. If $K^* = 0$, we will go to the next step. Otherwise, we propose a set of new parameters $\mathbf{a}_k^* = (a_{1k}^*, \dots, a_{nk}^*)^\top$ and w_{jk}^* from their prior distributions, $k = K + 1, \dots, K + K^*$. We accept new columns and the associated new parameters with probability

$$\min \left\{ 1, \frac{\prod_{i=1}^n p(z_{ij} | \{a_{ik}, b_{jk}, w_{jk}\}_{k=1}^K, \{a_{ik}^*, b_{jk}^*, w_{jk}^*\}_{k=K+1}^{K+K^*}, c_j)}{\prod_{i=1}^n p(z_{ij} | \{a_{ik}, b_{jk}, w_{jk}\}_{k=1}^K, c_j)} \right\},$$

where $b_{j,K+1} = \dots = b_{j,K+K^*} = 1$. Lastly, if new columns are accepted, we increase K by K^* and sample p_k for the new columns by a M-H step,

$$p(p_k|\mathbf{b}_k) \propto \{1 - (1 - p_k)^l\}(1 - p_k)^{l^*}/p_k.$$

To summarize the posterior distribution based on the Monte Carlo samples, we proceed by first calculating the maximum a posteriori estimate \widehat{K} of K from the marginal posterior distribution. Conditional on \widehat{K} , we find an estimate of \mathbf{B} by the following procedure. For any matrices $\mathbf{B}, \widetilde{\mathbf{B}} \in \{0, 1\}^{p \times \widehat{K}}$, we define a distance $d(\mathbf{B}, \widetilde{\mathbf{B}}) = \min_{\pi} H(\mathbf{B}, \pi(\widetilde{\mathbf{B}}))$, where $\pi(\widetilde{\mathbf{B}})$ denotes a permutation of the columns of $\widetilde{\mathbf{B}}$ and $H(\cdot, \cdot)$ is the Hamming distance between two binary matrices. A point estimator $\widehat{\mathbf{B}}$ of \mathbf{B} is then obtained as

$$\widehat{\mathbf{B}} = \arg \min_{\widetilde{\mathbf{B}}} \int d(\mathbf{B}, \widetilde{\mathbf{B}}) dp(\mathbf{B}|\cdot),$$

where $p(\mathbf{B}|\cdot)$ denotes the marginal posterior distribution of \mathbf{B} given K . Both the integration as well as the optimization can be approximated using the available Monte Carlo samples. Conditional on $\widehat{\mathbf{B}}$, we continue to run the chain for a short period. Then estimates of other parameters are obtained as posterior means computed from the new Monte Carlo samples. For example, to find the estimated binary matrix $\widehat{\mathbf{A}}$, we first compute the posterior probabilities of $a_{ik} = 1$ by averaging the Monte Carlo samples of \mathbf{A} . We then threshold the posterior probabilities to obtain $\widehat{\mathbf{A}}$. The threshold can be set at 0.5 as default or chosen in order to control the expected false discovery rate (Müller *and others*, 2006; Peterson *and others*, 2015). We remark that once conditional on $\widehat{\mathbf{B}}$, there is no label-switching issue in estimating the remaining parameters.

4. SIMULATION

In our simulation study, we consider a dataset with $n = 300$ hosts, $p = 46$ taxa, and $K = 6$ true clusters; similar in size to the later application. For $k = 1, \dots, K$, we first set $a_{ik} = 1$, $i = 60(k-1) + 1, \dots, 60k$, and 0 all the others. Then we randomly change 10% of zero entries in the host-cluster matrix \mathbf{A} to one. We use the same taxonomic rank tree as in later application to generate the taxon-cluster matrix \mathbf{B} , which has $L + 1 = 5$ levels (i.e., edge length $l = 0.25$). Furthermore, cluster-specific probability parameters p_k are all set to 0.3. The resulting true \mathbf{A} and \mathbf{B} , along with the phylogenetic tree are shown in Figure 1. Latent indicators z_{ij} are

generated from the logit model (2.3) with $\mathbf{w}_j = (2.0, 2.5, 3.0, 3.5, 4.0, 4.5)^\top$ and $c_j = \log 0.5$. For the unnormalized relative abundance γ_{ij} , we simulate them from the gamma mixture model (2.1) with varying degrees of separation of mixture components, $(s_j, t_j) = (s, t) = (2, 0.7)$, $(3, 0.6)$, and $(5, 0.5)$. Among these three simulation scenarios, $(s, t) = (2, 0.7)$ is the most difficult as it induces the least separation between the two mixture component. The observations are finally generated from the multinomial sampling model for which the total counts are drawn from the discrete uniform distribution $U(50, 500)$.

We run the MCMC algorithm of MMF for 5,000 iterations with 10 random initial clusters. The first 2,500 iterations are discarded as burn-in and posterior samples are retained every 5th iteration after burn-in. To evaluate recovery accuracy, we calculate the estimation errors for both \mathbf{A} and \mathbf{B} . Specifically, we compute the Hamming distance between the estimated and true \mathbf{A} and \mathbf{B} , normalized by the respective total number of elements. When the estimated number of clusters is different from the truth, we pad the smaller matrix with columns of zeros, making the resulting matrices comparable in dimension.

Method evaluation. The results under three sets of true values of (s, t) are summarized in Table 2 based on 50 repeated simulations. As expected, the method improves as the two mixture components in (2.2) become more separated, from $(s, t) = (2, 0.7)$ to $(5, 0.5)$. The proposed MMF is able to identify the correct number K of clusters at least 95% of the time. Figure 1 depicts the estimated host-cluster and taxon-cluster matrices $\hat{\mathbf{A}}$ and $\hat{\mathbf{B}}$ of the proposed MMF averaged over repeated simulations in the scenario $(s, t) = (5, 0.5)$, after adjusting for label switching and dropping redundant columns. They are visually quite close to the truth, indicating that the proposed method is able to consistently and accurately identify the clusters of hosts and taxa.

Comparisons with competing methods. Matrix factorization has been studied extensively in the literature. Here we compare the proposed MMF with three existing alternative matrix factorization methods, (i) the low rank approximation (LRA, Cao *and others* 2019b), the non-

negative matrix factorization (NNMF, Cai *and others* 2017), and the zero-inflated Poisson factor model (ZIPFM, Xu *and others* 2020).

In order to compare the performance of biclustering, the overlapping clustering method, fuzzy *c*-means (Bezdek *and others*, 1984), is applied to the latent factors or low rank matrices for the competing methods. The dimension of latent factors is chosen by their default optimization procedure. The number of clusters is set to the truth $K = 6$ for competing methods whereas it is estimated for the proposed MMF. The estimation errors are defined by first converting clustering results to binary host-cluster or taxon-cluster matrix, and then calculating the distance between the estimated and true matrices as is done for the proposed method. In addition, we also consider a two-step approach that is similar to the proposed MMF, denoted by TS. Specifically, instead of joint modeling, the two-step approach first dichotomizes observations using a default cutoff 0.25 quantile as suggested in Cai *and others* (2019) and then applies the same Bayesian nonparametric binary matrix factorization method as in MMF to the binary data. The results of all the methods are reported in Table 2. The proposed MMF consistently outperforms the competing methods in most settings (keeping in mind that the number of clusters is set to truth for LRA, NNMF, and ZIPFM), especially for the taxon-cluster matrix \mathbf{B} . Although when (s, t) is specified to be $(2, 0.7)$, the estimation error of \mathbf{A} in LRA is smaller, the significantly more accurate result of estimating \mathbf{B} in our proposed MMF shows the benefit of using the phylogenetic tree.

Sensitivity analyses. We perform two sets of sensitive analyses regarding the choice of hyperparameters as well as the impact of misspecified tree information. The inference under MMF is relatively robust. Details are provided in Supplementary Material (Section B).

5. REAL DATA

Gut microbes actively interact with their host and have profound relevance to IBD, which is a very heterogeneous disease at the microbiome level. The goal of this case study is to investigate

the heterogeneous microbial profiles in relation to IBD in an unsupervised data-driven manner. We apply the proposed MMF to an IBD microbiome dataset (Qin *and others*, 2010). The data are obtained by sequencing fecal specimens collected from IBD patients as well as healthy human adults using the Illumina’s Genome Analyzer (metagenomic sequencing); details of the data generating procedure can be found in Qin *and others* (2010). The dataset contains $n = 372$ observations with 240 healthy hosts and 132 IBD patients, and provides information on microbial contents at various taxonomic levels (kingdom, phylum, class, order, family, genus and specie) of these samples. We choose to work with the family level counts because lower levels (genus and specie) have extremely large number of zeros (more than 80% elements in the count matrix are zeros). In addition, we filter out families that appear in less than 10% of samples (i.e. taxa with more than 90% of zeros) and preserve only families belonging to kingdom bacteria. The resulting data have $p = 46$ taxa to be used for subsequent analysis. The relationships of taxa can be naturally represented by a taxonomic rank tree. Taxa that are closer on the tree tend to have similar activities, abundance, and functions. We depict the tree of 46 taxa along with their higher taxonomic ranks, kingdom, phylum, class, and order in Figure 4. This taxonomic rank tree will be used as prior information to encourage the clustering of taxa that are taxonomically similar.

We run two separate MCMCs of MMF for 10,000 iterations. The first 5,000 iterations are discarded as burn-in and posterior samples are retained every 5th iteration after burn-in. To monitor the MCMC convergence, we compute the Gelman and Rubin’s potential scale reduction factor (PSRF, Gelman and Rubin, 1992) for key parameters. The MCMC diagnostic does not show a sign of lack of convergence: the PSRF is 1.01 for number K of clusters and the median PSRF is < 1.1 (with stdev 0.1) for $c_j + \sum_{k=1}^K a_{ik} w_{jk} b_{jk}$, the quantity on the right-hand side of (2.3). The Monte Carlo samples from the two Markov chains are combined for subsequent analysis.

To check the model fit adequacy, we perform within-sample prediction that compare the

observed composition (i.e. \mathbf{x}_i/N_i) with the posterior predictive mean. The scatter plot of predicted versus observed relative abundance of taxa is given in Figure 2a showing that the within-sample prediction is accurate. The correlation between two matrices is 0.94, which indicates an adequate model fit.

We now report the results from posterior inference. Figure 2b shows the posterior distribution of the number K of clusters. The posterior mode occurs at $K = 6$. Conditional on K , the posterior estimates of \mathbf{A} and \mathbf{B} are shown in Figure 4. In Figure 4a, black cells are 0, green cells are 1 for controls, and red cells are 1 for patients. Samples that do not belong to any clusters are omitted in the figure. To visualize the neighboring relationships of the hosts in a low dimensional space, we depict the t -distributed stochastic neighbor embedding plot (t-SNE) in Figure 3. It shows that hosts who do not belong to any clusters locate on the periphery of the plot.

Cluster 1 is predominantly IBD patients, accounted for about 70%. The bi-clustering nature of the proposed MMF allows us to investigate the corresponding subset of taxa that are related to these IBD patients. For example, the cluster 1 contains family *Enterobacteriaceae*, part of class *Gammaproteobacteria*, which have been reported to increase in relative abundance in patient with IBD (Lupp *and others*, 2007). The fact that it exclusively belongs to patient-dominated cluster 1 is consistent with its biological relevance to IBD. Moreover, genus *Fusobacterium*, a member of the family *Fusobacteriaceae*, have been found to be at a higher abundance in patients with ulcerative colitis (UC, a subtype of IBD) relative to control subjects (Ohkusa *and others*, 2002). *Fusobacteriaceae* family is also contained in cluster 1 only, which again signifies the importance of this family with relevance to IBD. Generally, phyla *Proteobacteria* and *Actinobacteria* are expected to increase in IBD patients (Matsuoka and Kanai, 2015), which is consistent with our result in cluster 1. Apart from the findings that are confirmed by the existing literature, cluster 1 includes some families in phylum *Firmicutes*, which are known to play major anti-inflammatory roles and therefore their abundances are expected to decrease in IBD patients. Further biological

investigation is required to validate this new finding.

Likewise, most of hosts in cluster 6 are IBD patients as well. But they are associated with a different set of taxa. For example, it contains the family *Pasteurellaceae*, of which the abundances tend to increase in patients with Crohn's disease (CD, Gevers *and others*, 2014), another subtype of IBD,.

Cluster 2 is dominated by normal samples. It is associated with genera *Bifidobacterium* and *Faecalibacterium*, members of families *Bifidobacteriaceae* and *Ruminococcaceae*, which have been shown to be protective of the host from inflammation via several mechanisms (Sokol *and others*, 2008), including the stimulation of the anti-inflammatory cytokine IL-10 and down-regulation of inflammatory cytokines. A reduced abundance of genus *Odoribacter*, which belongs to family *Porphyromonadaceae* is discovered in the most severe form of UC, pancolitis (Morgan *and others*, 2012). It also contains class *Betaproteobacteria*, of which the relationship with IBD is yet to establish.

Cluster 3, 4, and 5 have a mix of patients and controls. It contains genera *Bacteroides* and *Roseburia*, belongs to families *Bacteroidaceae* and *Lachnospiraceae*, respectively. They have been shown to decrease in IBD patients (Machiels *and others*, 2014; Zhou and Zhi, 2016).

We have reported results are confirmed by the biological literature. Our result also provides novel insight into the relationship between microbes and IBD that are revealed by biclustering structure, which need to be further verified by biological experiments. Our discoveries are potentially useful as a guidance to design and conduct more targeted and focused experiments.

For comparison, we apply MMF without the tree information (i.e., using the ordinary IBP prior) to this dataset. The result is shown in Figure 5. It identifies 4 clusters, and most clusters are dominated by control samples. Without tree information, we fail to identify the cluster associated with IBD patients and two associated bacteria families *Enterobacteriaceae* and *Fusobacteriaceae*, which are successfully discovered when prior biological knowledge regarding the taxonomic ranks

are incorporated in the analysis. Additionally, taxa from the same cluster are much less similar taxonomically: the log probability of generating this matrix from the taxonomic tree is -119.95 , whereas the log probability of generating the matrix inferred from the pIBP is -91.48 , which indicates that the results from the pIBP prior are substantially more consistent with the taxonomic rank tree. Without using the tree information, the lack of taxonomic similarity within the identified clusters makes it hard to interpret the results biologically.

6. DISCUSSION

In this paper, we developed a novel identifiable sparse MMF method to simultaneously cluster microbes and hosts. The proposed approach accounts for the compositional, sparse, heterogeneous, and noisy nature of microbiome data, and describes the data generating process by a hierarchical Bayesian model, which allows for probabilistic characterization of latent structures (i.e., overlapping clusters) through full posterior inference. In microbiome data, the incorporation of taxonomic knowledge greatly facilitates the interpretability and reproducibility of the inferred clusters. Our simulation results demonstrate the advantage of utilizing prior information to assist inference on latent clusters. In analyzing a gut microbiome dataset, we find latent microbial communities that are closely related to IBD and its subtypes.

There are four directions that can be taken to extend this work. First, zero-inflation exists in other data types such as single-cell RNA-seq data. It is far less common to treat single-cell data as multinomial counts and therefore the proposed MMF cannot be directly applied. However, with a minor modification of the sampling distribution (e.g. zero-inflated Poisson distribution), the method can be generalized for biclustering single-cell data. Second, the joint modeling approach can be used for many other tasks beyond matrix factorization. For example, microbial networks can be inferred by replacing the matrix factorization model with a graphical model (e.g. Markov random fields or Bayesian networks) on the latent binary indicators \mathbf{Z} . Third, MCMC allows

for full posterior inference but is not scalable to large and high-dimensional data. The current inference algorithm can be substantially accelerated by using consensus Monte Carlo algorithms for big-data clustering (Ni *and others*, 2019a) without sacrificing much accuracy. Fourth, the overlapping clusters can be restricted to non-overlapping clusters if desired by considering random partition models including various extensions of the Dirichlet process (Lijoi *and others*, 2007; Favaro and Teh, 2013; De Blasi *and others*, 2013).

7. SOFTWARE

Software in the form of R code, together with a complete documentation is available on request from the first author (fangtingzhou@tamu.edu). The data that support the findings of this study are openly available in the R package `curatedMetagenomicData` which can be downloaded at <https://github.com/waldronlab/curatedMetagenomicData/>.

8. SUPPLEMENTARY MATERIAL

Supplementary material is available online at <http://biostatistics.oxfordjournals.org>.

REFERENCES

- BENHADOU, FARIDA, MINTOFF, DILLON, SCHNEBERT, BENJAMIN AND THIO, HOK BING. (2018). Psoriasis and microbiota: a systematic review. *Diseases* **6**(2), 47.
- BEZDEK, JAMES C, EHRLICH, ROBERT AND FULL, WILLIAM. (1984). FCM: The fuzzy c-means clustering algorithm. *Computers & Geosciences* **10**(2-3), 191–203.
- BHATTACHARYA, ANIRBAN AND DUNSON, DAVID B. (2011). Sparse Bayesian infinite factor models. *Biometrika*, 291–306.
- BISHOP, CHRISTOPHER. (2006). *Pattern recognition and machine learning*. New York: Springer.

- BUCCIANTI, ANTONELLA. (2013). Is compositional data analysis a way to see beyond the illusion? *Computers & Geosciences* **50**, 165–173.
- CAI, TONY, LI, HONGZHE, MA, JING AND XIA, YIN. (2019). Differential Markov random field analysis with an application to detecting differential microbial community networks. *Biometrika* **106**(2), 401–416.
- CAI, YUN, GU, HONG AND KENNEY, TOBY. (2017). Learning microbial community structures with supervised and unsupervised non-negative matrix factorization. *Microbiome* **5**, 110.
- CAO, YUANPEI, LIN, WEI AND LI, HONGZHE. (2019a). Large covariance estimation for compositional data via composition-adjusted thresholding. *Journal of the American Statistical Association* **114**(526), 759–772.
- CAO, YUANPEI, ZHANG, ANRU AND LI, HONGZHE. (2019b). Multisample estimation of bacterial composition matrices in metagenomics data. *Biometrika* **107**(1), 75–92.
- CASTANER, OLGA *and others*. (2018). The gut microbiome profile in obesity: a systematic review. *International Journal of Endocrinology* **2018**.
- CHEN, ERIC Z AND LI, HONGZHE. (2016). A two-part mixed-effects model for analyzing longitudinal microbiome compositional data. *Bioinformatics* **32**(17), 2611–2617.
- CHEN, JUN AND LI, HONGZHE. (2013). Variable selection for sparse Dirichlet-multinomial regression with an application to microbiome data analysis. *Ann. Appl. Stat.* **7**(1), 418–442.
- CHEN, MENGJIE, GAO, CHAO AND ZHAO, HONGYU. (2016). Posterior contraction rates of the phylogenetic Indian buffet processes. *Bayesian Analysis* **11**(2), 477–497.
- DE BLASI, PIERPAOLO, FAVARO, STEFANO, LIJOI, ANTONIO, MENA, RAMSÉS H, PRÜNSTER, IGOR AND RUGGIERO, MATTEO. (2013). Are Gibbs-type priors the most natural generalization of the Dirichlet process? *IEEE Trans. Pattern Anal. Mach. Intell.* **37**(2), 212–229.

- FAVARO, STEFANO AND TEH, YEE WHYEE. (2013). MCMC for normalized random measure mixture models. *Statistical Science* **28**(3), 335–359.
- FETTWEIS, JENNIFER M *and others*. (2019). The vaginal microbiome and preterm birth. *Nature Medicine* **25**(6), 1012–1021.
- FRANZOSA, ERIC A *and others*. (2019). Gut microbiome structure and metabolic activity in inflammatory bowel disease. *Nature Microbiology* **4**(2), 293–305.
- FRIEDMAN, JONATHAN AND ALM, ERIC J. (2012). Inferring correlation networks from genomic survey data. *PLoS Computational Biology* **8**(9), e1002687.
- GELMAN, ANDREW AND RUBIN, DONALD B. (1992). Inference from iterative simulation using multiple sequences. *Statistical Science* **7**(4), 457–472.
- GEVERS, DIRK *and others*. (2014). The treatment-naïve microbiome in new-onset crohn’s disease. *Cell Host & Microbe* **15**(3), 382–392.
- GLOOR, GREGORY B *and others*. (2017). Microbiome datasets are compositional: and this is not optional. *Frontiers in Microbiology* **8**, 2224.
- GOPALAN, PREM *and others*. (2014). Bayesian nonparametric Poisson factorization for recommendation systems. In: *AISTATS*, Volume 33. pp. 275–283.
- GRIFFITHS, THOMAS L AND GHAHRAMANI, ZOUBIN. (2005). Infinite latent feature models and the Indian buffet process. In: *NIPS*. pp. 475–482.
- HOYER, PATRIK O. (2004). Non-negative matrix factorization with sparseness constraints. *Journal of Machine Learning Research* **5**, 1457–1469.
- LEE, DANIEL D AND SEUNG, H SEBASTIAN. (2000). Algorithms for non-negative matrix factorization. In: *NIPS*. pp. 535–541.

- LIJOI, ANTONIO, MENA, RAMSÉS H AND PRÜNSTER, IGOR. (2007). Controlling the reinforcement in Bayesian non-parametric mixture models. *J. R. Stat. Soc. B* **69**(4), 715–740.
- LIN, WEI, SHI, PIXU, FENG, RUI AND LI, HONGZHE. (2014). Variable selection in regression with compositional covariates. *Biometrika* **101**(4), 785–797.
- LIU, LEI *and others*. (2019). Statistical analysis of zero-inflated nonnegative continuous data: A review. *Statistical Science* **34**(2), 253–279.
- LLOYD-PRICE, JASON *and others*. (2019). Multi-omics of the gut microbial ecosystem in inflammatory bowel diseases. *Nature* **569**(7758), 655–662.
- LUPP, CLAUDIA *and others*. (2007). Host-mediated inflammation disrupts the intestinal microbiota and promotes the overgrowth of enterobacteriaceae. *Cell Host & Microbe* **2**(2), 119–129.
- MACHIELS, KATHLEEN *and others*. (2014). A decrease of the butyrate-producing species *Roseburia hominis* and *Faecalibacterium prausnitzii* defines dysbiosis in patients with ulcerative colitis. *Gut* **63**(8), 1275–1283.
- MATSUOKA, KATSUYOSHI AND KANAI, TAKANORI. (2015). The gut microbiota and inflammatory bowel disease. In: *Seminars in Immunopathology*, Volume 37. pp. 47–55.
- MEEDS, EDWARD, GHARAMANI, ZOUBIN, NEAL, RADFORD M AND ROWEIS, SAM T. (2007). Modeling dyadic data with binary latent factors. In: *NIPS*. pp. 977–984.
- MILLER, KURT T, GRIFFITHS, THOMAS L AND JORDAN, MICHAEL I. (2008). The phylogenetic Indian buffet process: a non-exchangeable nonparametric prior for latent features. In: *Proceedings of the 24th Conference on Uncertainty in Artificial Intelligence*. pp. 403–410.
- MORGAN, XOCHITL C *and others*. (2012). Dysfunction of the intestinal microbiome in inflammatory bowel disease and treatment. *Genome Biology* **13**(9), R79.

- MÜLLER, PETER, PARMIGIANI, GIOVANNI AND RICE, KENNETH. (2006). FDR and Bayesian multiple comparisons rules. In: *Proceedings of the 8th Valencia World Meeting on Bayesian Statistics*. Oxford University Press.
- NI, YANG, MÜLLER, PETER, DIESENDRUCK, MAURICE, WILLIAMSON, SINEAD, ZHU, YITAN AND JI, YUAN. (2019a). Scalable Bayesian nonparametric clustering and classification. *Journal of Computational and Graphical Statistics*, 1–13.
- NI, YANG, MÜLLER, PETER AND JI, YUAN. (2019b). Bayesian double feature allocation for phenotyping with electronic health records. *J. Am. Stat. Assoc.*, 1–15.
- OHKUSA, TOSHIFUMI *and others*. (2002). Fusobacterium varium localized in the colonic mucosa of patients with ulcerative colitis stimulates species-specific antibody. *J. Gastroenterol. Hepatol.* **17**(8), 849–853.
- PETERSON, CHRISTINE, STINGO, FRANCESCO C AND VANNUCCI, MARINA. (2015). Bayesian inference of multiple Gaussian graphical models. *J. Am. Stat. Assoc.* **110**(509), 159–174.
- QIN, JUNJIE *and others*. (2010). A human gut microbial gene catalogue established by metagenomic sequencing. *Nature* **464**(7285), 59–65.
- ROČKOVÁ, VERONIKA AND GEORGE, EDWARD I. (2016). Fast Bayesian factor analysis via automatic rotations to sparsity. *J. Am. Stat. Assoc.* **111**(516), 1608–1622.
- SHI, PIXU, ZHANG, ANRU AND LI, HONGZHE. (2016). Regression analysis for microbiome compositional data. *The Annals of Applied Statistics* **10**(2), 1019–1040.
- SOKOL, HARRY *and others*. (2008). Faecalibacterium prausnitzii is an anti-inflammatory commensal bacterium identified by gut microbiota analysis of crohn disease patients. *Proceedings of the National Academy of Sciences* **105**(43), 16731–16736.

- TILG, HERBERT AND MOSCHEN, ALEXANDER R. (2014). Microbiota and diabetes: an evolving relationship. *Gut* **63**(9), 1513–1521.
- TURNBAUGH, PETER J *and others*. (2007). The human microbiome project. *Nature* **449**, 804–810.
- WATTS, STEPHEN C, RITCHIE, SCOTT C, INOUE, MICHAEL AND HOLT, KATHRYN E. (2018). FastSpar: rapid and scalable correlation estimation for compositional data. *Bioinformatics* **35**(6), 1064–1066.
- WOOD, FRANK, GRIFFITHS, THOMAS L AND GHARAMANI, ZOUBIN. (2006). A non-parametric bayesian method for inferring hidden causes. In: *UAI*. pp. 536–543.
- WU, ZHENKE, CASCIOLA-ROSEN, LIVIA, ROSEN, ANTONY AND ZEGER, SCOTT L. (2019). A Bayesian approach to restricted latent class models for scientifically-structured clustering of multivariate binary outcomes. *bioRxiv*.
- XU, TIANCHEN, DEMMER, RYAN T. AND LI, GEN. (2020). Zero-inflated poisson factor model with application to microbiome read counts. *Biometrics* **n/a**(n/a), just-accepted.
- ZHOU, MINGYUAN, HANNAH, LAUREN, DUNSON, DAVID AND CARIN, LAWRENCE. (2012). Beta-negative binomial process and Poisson factor analysis. In: *Proceedings of the Fifteenth International Conference on Artificial Intelligence and Statistics*, Volume 22. pp. 1462–1471.
- ZHOU, YINGTING AND ZHI, FACHAO. (2016). Lower level of bacteroides in the gut microbiota is associated with inflammatory bowel disease: a meta-analysis. *BioMed Research International* **2016**.

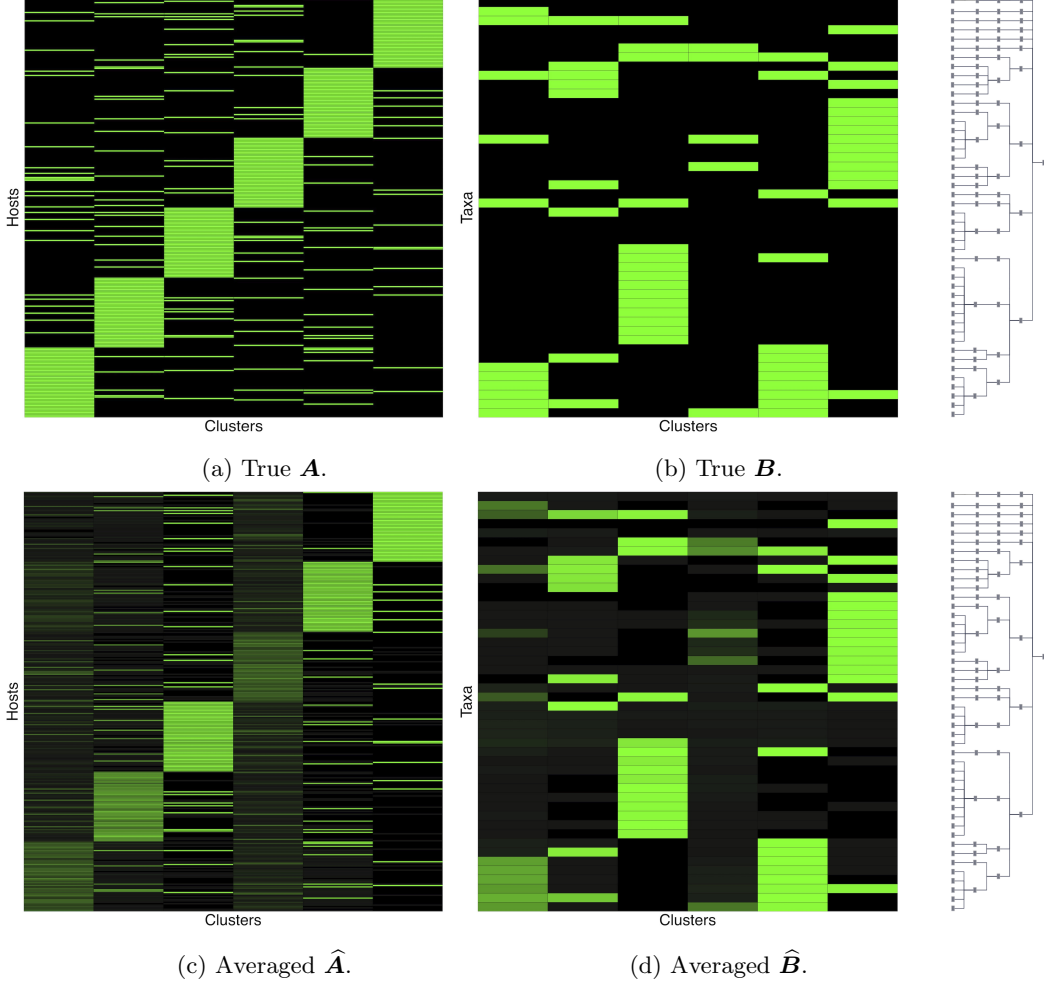


Fig. 1: Accuracy evaluation. Panels (a)&(b). True values of \mathbf{A} and \mathbf{B} used to generate the simulated data. Green cells are ones and black cells are zeros. Panels (c)&(d). The average estimated $\hat{\mathbf{A}}$ and $\hat{\mathbf{B}}$ over 50 replicates with parameters $(s, t) = (5, 0.5)$. The color of cells change gradually from black to green representing values from 0 to 1. Note that they take values between 0 and 1 because they are averaged over repeat simulations. The columns of \mathbf{B} and $\hat{\mathbf{B}}$ are ordered according to the taxonomic rank tree.

Table 1: Summary of the complete hierarchical model.

Multinomial sampling	$\mathbf{x}_i \sim \text{Multinomial}(N_i, \boldsymbol{\pi}_i)$ with $\boldsymbol{\pi}_i = \boldsymbol{\gamma}_i / \sum_{j=1}^p \gamma_{ij}$
Mixture representation of the composition	$\gamma_{ij} \sim z_{ij} \text{Gamma}(s_j, 1) + (1 - z_{ij}) \text{Gamma}(t_j, 1)$ $(s_j, t_j) \sim p(s_j, t_j) = \text{Gamma}(s_j \alpha_s, \beta_s)$ $\times \text{Gamma}(t_j \alpha_t, \beta_t) \times \mathbf{I}(s_j > t_j)$
Latent matrix factorization	$\text{logit}\{\text{Pr}(z_{ij} = 1)\} = c_j + \sum_{k=1}^K a_{ik} w_{jk} b_{jk}$ $\mathbf{B} \sim \text{pIBP}(\alpha)$, $a_{ik} \sim \text{Bernoulli}(\rho)$, $\rho \sim \text{Beta}(\alpha_\rho, \beta_\rho)$ $w_{jk} \sim \text{Gamma}(\alpha_w, \beta_w)$, $c_j \sim \text{N}(\mu_c, \sigma_c)$

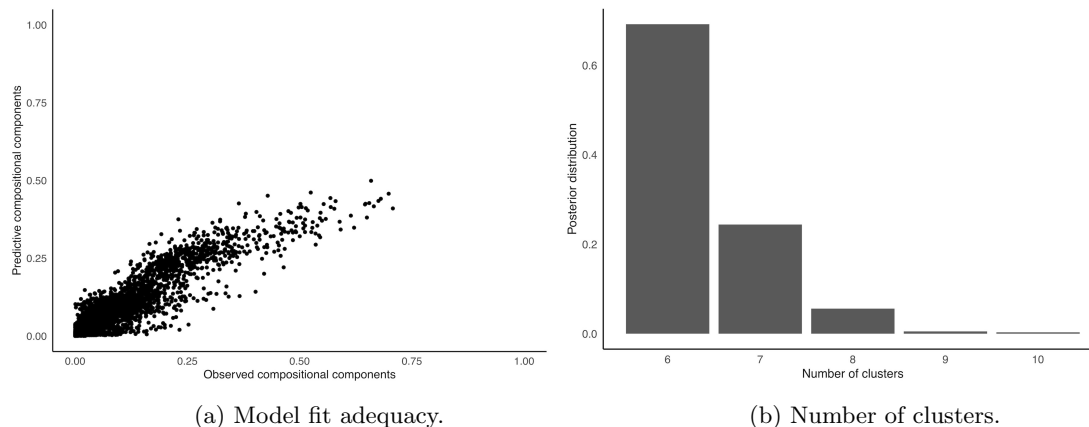


Fig. 2: Real data. (a) Scatter plot of observed (x -axis) and posterior predictive (y -axis) relative abundance of taxa in hosts. (b) Posterior distribution of the number of clusters.

Table 2: Simulation results of the proposed MMF and competing methods. Average errors in estimating \mathbf{A} and \mathbf{B} are quantified as the Hamming distance between the estimated and true \mathbf{A} and \mathbf{B} , normalized by the respective total number of elements. The numbers in the parentheses are standard deviations. The smallest errors are in boldface. The competing methods are low rank approximation (LRA), non-negative matrix factorization (NNMF), zero-inflated Poisson factor model (ZIPFM), and two-step multinomial matrix factorization (TS).

(s, t)	(2, 0.7)		(3, 0.6)		(5, 0.5)	
	Error \mathbf{A}	Error \mathbf{B}	Error \mathbf{A}	Error \mathbf{B}	Error \mathbf{A}	Error \mathbf{B}
MMF	0.373 (0.062)	0.167 (0.029)	0.171 (0.022)	0.055 (0.021)	0.117 (0.023)	0.057 (0.028)
LRA	0.298 (0.042)	0.269 (0.023)	0.205 (0.052)	0.185 (0.017)	0.203 (0.058)	0.165 (0.021)
NNMF	0.351 (0.049)	0.279 (0.030)	0.288 (0.062)	0.247 (0.021)	0.256 (0.059)	0.208 (0.014)
ZIPFM	0.425 (0.014)	0.258 (0.031)	0.291 (0.008)	0.249 (0.023)	0.246 (0.002)	0.232 (0.022)
TS	0.382 (0.092)	0.253 (0.033)	0.325 (0.057)	0.132 (0.043)	0.237 (0.092)	0.089 (0.018)

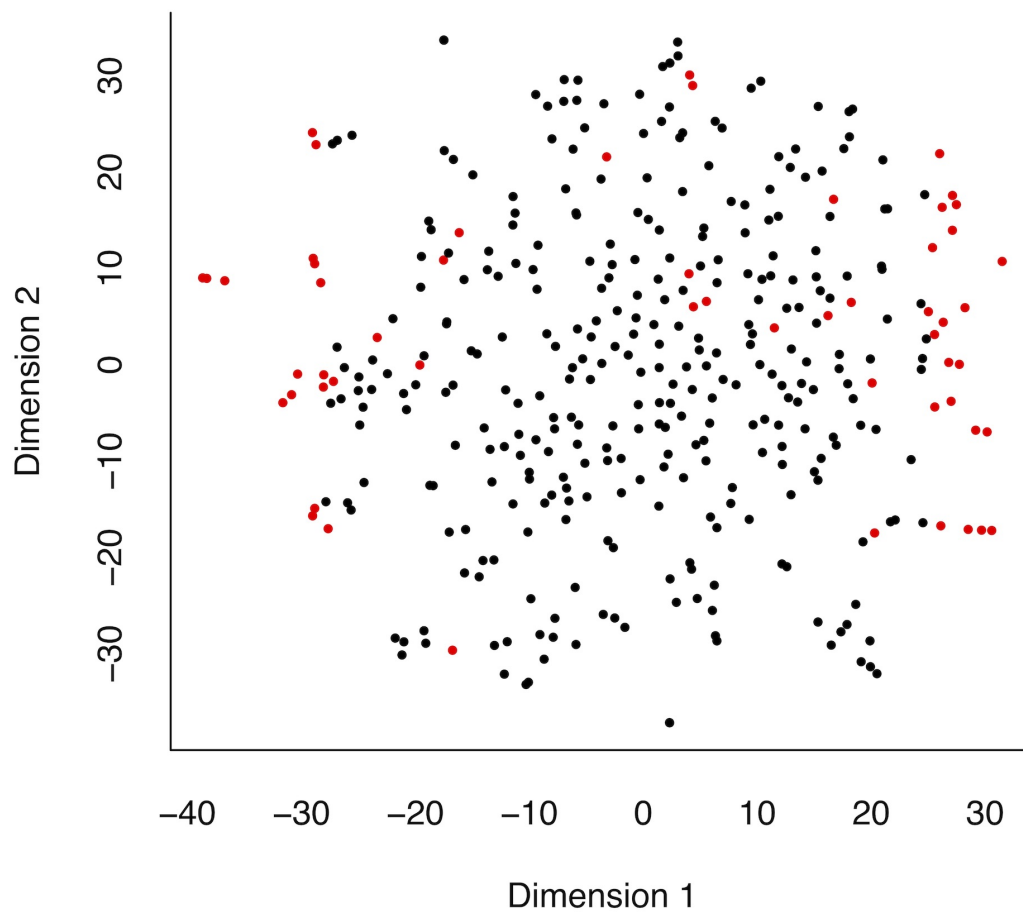


Fig. 3: t-SNE plot of hosts in two dimensional space. Red points are samples that do not belong to any clusters.

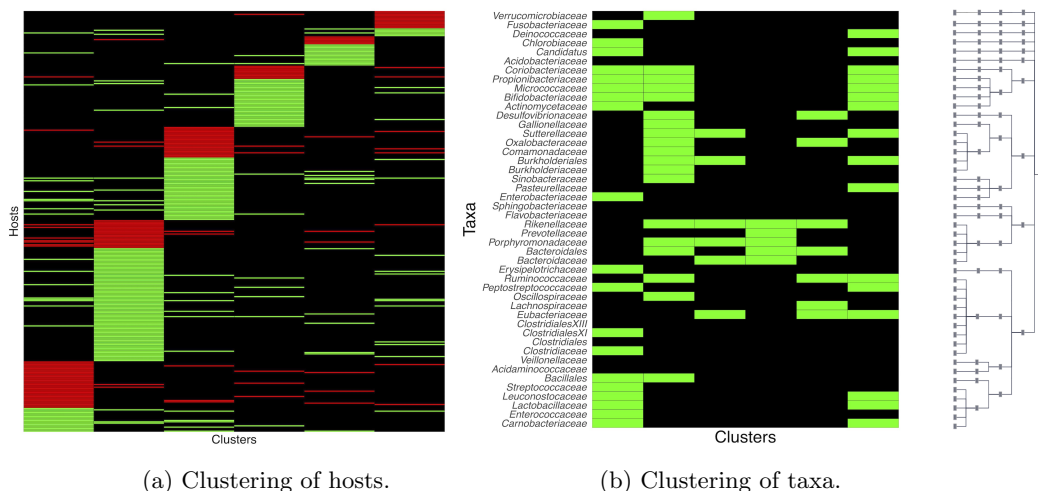


Fig. 4: Real data. Heatmaps of estimated clusters using the proposed MMF. Colored cells are ones and black cells are zeros. Rows of \mathbf{A} are hosts arranged in a block-diagonal-liked form. Rows of \mathbf{B} are taxa which are arranged according to the taxonomic rank tree. Each column represents a cluster with overlaps. The red/green cells in the heatmap of \mathbf{A} represents patients/controls with ones.

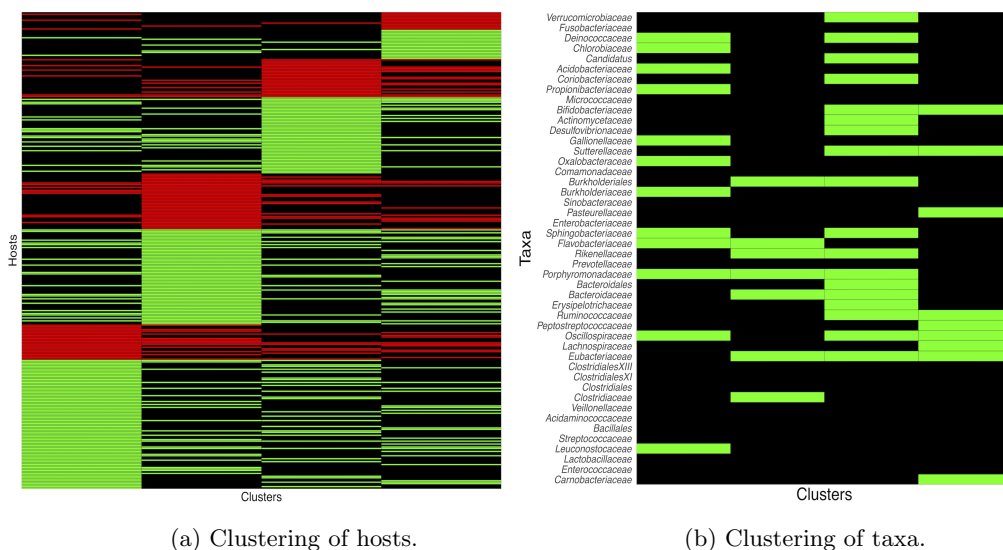


Fig. 5: Real data. Heatmaps of estimated clusters using the ordinary IBP prior. Colored cells are ones and black cells are zeros. Rows of \mathbf{A} are hosts arranged in a block-diagonal-liked form. Rows of \mathbf{B} are taxa which are arranged according to the taxonomic rank tree. Each column represents a cluster with overlaps. The red/green cells in the heatmap of \mathbf{A} represents patients/controls with ones.